Environmental Research 286 (2025) 122851

Contents lists available at ScienceDirect

Environmental Research

journal homepage: www.elsevier.com/locate/envres

Carbon dots as dual-action nanotools for metal toxicity recognition and mitigation

Inês Domingues [a,*], João Amaral [b], Bruna Vieira [b], Ana Luísa Machado [a], Carla I.M. Santos [c,d], Joana P.M. Sousa [e,f], Alice Sciortino [g], Roberta Cillari [h], Radian Popescu [i], Yolita M. Eggeler [i], Fabrizio Messina [g], Nicolò Mauro [h], Gil Gonçalves [f,j]

[a] CESAM and Department of Biology, University of Aveiro, Campus Universitário de Santiago, 3810-193, Aveiro, Portugal
[b] Department of Biology, University of Aveiro, Campus Universitário de Santiago, 3810-193, Aveiro, Portugal
[c] Centro de Química Estrutural (CQE), Instituto Superior Técnico, Av. Rovisco Pais, 1049-001 Lisboa, Portugal
[d] LAQV-REQUIMTE, Department of Chemistry, University of Aveiro, Campus Universitário de Santiago, 3810-193 Aveiro, Portugal
[e] CICECO, Chemistry Department, University of Aveiro, Campus Universitário de Santiago, 3810-193, Aveiro, Portugal
[f] Centre for Mechanical Technology and Automation (TEMA), Mechanical Engineering Department, University of Aveiro, 3810-193 Aveiro, Portugal
[g] Dipartimento di Fisica e Chimica – Emilio Segrè, Università degli Studi di Palermo, Via Archirafi 36, 90123 Palermo, Italy
[h] Laboratory of Biocompatible Polymers, Department of Biological, Chemical, and Pharmaceutical Sciences and Technologies (STEBICEF), University of Palermo, via Archirafi 32, 90123 Palermo, Italy
[i] Karlsruhe Institute of Technology, Laboratory for Electron Microscopy, Engesserstr. 7, 76131 Karlsruhe, Germany
[j] Intelligent Systems Associate Laboratory (LASI), 4800-058 Guimarães, Portugal

ARTICLE INFO

Keywords:
Danio rerio
Carbon nanodots
Fluorescence imaging
Metallic ions
Adsorption

ABSTRACT

Carbon dots (CDs) have emerged as promising agents for mitigating metal toxicity and monitoring metal contamination in aquatic environments. This study investigated the dual functionality of CDs as anti-toxicity agents and biosensors for cadmium (Cd^{2+}), nickel (Ni^{2+}), and silver (Ag^{+}) in a zebrafish embryo model. Zebrafish embryos were exposed to various concentrations of CDs (0, 5, and 50 mg L^{-1}) in combination with different metal concentrations. Toxicity was assessed by measuring the lethality, hatching rate, swimming activity, and AChE activity. CDs significantly reduced the lethal toxicity of all tested metals, with LC_{50} values increasing from 56.0 to 110.0 μM for Cd^{2+}, 0.4–1.6 μM for Ag^{+}, and becoming undeterminable for Ni^{2+} at the highest CDs concentration. Photophysical characterization revealed that the CDs exhibited metal-specific fluorescence, enabling the development of an optical fingerprint for metal identification. Fluorescence imaging of zebrafish embryos demonstrated the effectiveness of CDs as *in vivo* tracers of metallic contaminants, highlighting their utility in studying biological processes. These findings highlight the dual functionality of CDs as agents to reduce metal toxicity and as monitoring tools for water quality assessment, making them a versatile solution for addressing metal contamination challenges in aquatic and biological systems.

Environmental implications: The present study explores the potential of carbon dots as nanotools for water remediation. Carbon dots have a high absorption capacity and can remove several compounds, including metals, from aquatic environments. This is highly relevant because contamination by metallic compounds is an environmental concern and that technology is constantly being sought to minimize the impact of these compounds on aquatic systems. Due to natural fluorescence which can be changed by metallic ions, carbon dots also show potential for monitoring aquatic contamination contributing as a potential tool in risk assessment strategies.

1. Introduction

Environmental pollution results mostly from anthropogenic activities fueled by exponential population and economic growth, leading to disturbances in the natural balance of the environment (Masindi et al., 2018; Tang et al., 2021). Metals are a subclass of inorganic pollutants that have harmful effects on the environment, even at very low concentrations, by bioaccumulating in living organisms and exerting toxic

* Corresponding author.
E-mail address: inesd@ua.pt (I. Domingues).

https://doi.org/10.1016/j.envres.2025.122851
Received 21 March 2025; Received in revised form 9 September 2025; Accepted 11 September 2025
Available online 12 September 2025

effects at several levels (Herawati et al., 2000). Therefore, the development of biocompatible detoxification strategies for these common pollutants is extremely important and represents a hot topic in nanotechnology. Metals occur naturally in the crust of the planet; however, the anthropogenic use of these compounds has dramatically increased, leading to a significant increase in their levels, especially in aquatic systems (Järup, 2003). Important sources of metals release into the environment are acid drainage from mining activities (Bradl, 2005), emission of gases into the atmosphere from thermoelectric plants, intensive agriculture practices using pesticides containing metals like Cd, Hg, and Pb (which are carried into the groundwater and adjacent bodies of water by rain and irrigation) (Gimeno-García et al., 1996). The effects of metals are perceptible even at low concentrations and affect several physiological and biochemical processes (Järup, 2003). Multiple pathways contribute to the toxicity of metals in organisms, including the disruption of enzymatic processes, generation of reactive oxygen species (ROS), effects on ion control levels, and effects on DNA and protein synthesis (Hartwig, 2013).

Recent advances in water remediation have focused on the development of holistic approaches, emphasizing complex mixtures rather than a small set of regulated, well-known chemicals that have been studied for decades (Ferraro and Prasse, 2021). Consequently, it is necessary to integrate the development of high-performance nanostructured sorbents, bioassays, real-time sensing of complex chemical mixtures, and artificial intelligence (Tran et al., 2023a). This integration will allow the development of a radically different approach to ensure water safety and quality. Carbon dots (CDs), an emerging class of zero-dimensional carbon-based nanomaterials with quasi-spherical shapes and diameters below 10 nm (Đorđević et al., 2022), can sense or remediate water contaminants (Tran et al., 2023b; Rasheed et al., 2023). Their hybrid structure, mostly composed of carbon, oxygen and nitrogen atoms, offers a great versatility for interacting with several different atoms, molecules and macromolecules (Arcudi and Đorđević, 2023). In addition, CDs offer excellent biocompatibility, a high quantum yield, good water dispersibility, and tunable excitation under different chemical or physical stimuli (Hoang et al., 2023a; Minh Hoang et al., 2024). It has been noted that the functional groups of CDs, particularly those containing oxygen components, have an affinity for specific pollutants. As a result, this affinity causes alterations in CDs optical properties, including the suppression or enhancement of fluorescence and shifts in the emission wavelength (Zhang et al., 2022). Fluorescence spectroscopy of CDs has been widely used to determine the exact quenching mechanism based on changes in the fluorescence intensity and lifetime (Hola et al., 2014; Wang et al., 2017a). Different primary mechanisms of quenching can occur in CDs (Simões et al., 2024), comprising Surface Energy Transfer (SET) (Ajith et al., 2022) and Photoinduced Electron Transfer (PET) (Wang et al., 2017b). Several studies have highlighted the use of CDs as effective probes for detecting single metal ions at low limit of detection (LOD), including Ag^{+} (LOD of 4.7 μM) (Wang et al., 2023), Ni^{2+} (LOD 3.14 μM) (Phetcharee et al., 2021), for Fe^{3+} (LOD of 3.95 μM) (Han et al., 2016) and Cd^{2+} (LOD of 0.000150 μM (Gu et al., 2018), among others (López-Beltrán et al., 2023; Torres Landa et al., 2022). However, it is important to note that the selective detection of metal ions must be modulated by controlling the type and density of CDs surface functional groups (Hu et al., 2024). For instance, carboxylated-CDs have been successfully explored to detect multiple metal ions in mineral water and tap water samples, including Fe^{3+}, Pb^{2+}, and Hg^{2+} (Hoang et al., 2023b)' (Li et al., 2017).

In addition to their probe potential, CDs can act as highly efficient agents for metals remediation in aquatic environments owing to their excellent adsorption capacity and high surface-to-volume ratio, thus providing an advantage over conventional sorbents (Ajith et al., 2022; Ikram et al., 2024). Adsorption is mainly governed by chemisorption and physisorption (Bhattacharjee et al., 2023). These distinct mechanisms enable CDs to effectively bind to and remove metal ions from aqueous environments. During chemical adsorption, various types of interactions can occur between CDs and metals, such as ion exchange and complexation, and in some cases, covalent bonding (Tan et al., 2022). In the case of physical adsorption, interactions can involve van der Waals forces, dipole-dipole interactions, or electrostatic interactions. In recent years, numerous studies have demonstrated the potential of CDs as effective adsorbents for metal contamination. For instance, CDs have already shown a high removal efficiency (RE) on remediation of multiple metal ions such as Cu^{2+} (RE = 37 %) and Pb^{2+} (RE = 75 %) (Sabet and Mahdavi, 2019a), Fe^{3+} (RE = 74 %) and Ni^{2+} (RE = 79 %) (Ajith et al., 2020a), including highly complex mixtures of Hg^{2+} (RE = 99 %), Cd^{2+} (RE = 82 %), Cr^{3+} (RE = 72 %), and Pb $^{2+}$ (RE = 80 %) (Perumal et al., 2022).

The biosafety of CDs to *in vivo* models such as zebrafish (*Danio rerio*) embryos has been confirmed by several authors (Umar et al., 2023; Huang et al., 2018; Liu et al., 2020; Chung et al., 2021). For instance, Liu et al. evaluated the morphological, developmental, behavioral, and histological changes in zebrafish larvae after five days of exposure to CDs and concluded that CDs could be safely utilized at concentrations below 200 mg L^{-1}. Bai et al. recently reviewed the effects of CDs on zebrafish and found the effects of exposure to very high CDs concentrations (hundreds of milligrams per liter) (Bai and Tang, 2023). The zebrafish model has been extensively utilized to assess the ability of CDs to detect various metals through variations in fluorescence emission, including Hg^{2+}, Cu^{2+}, Co^{2+}, Ni^{2+}, Ce^{3+}, Mn^{2+}, Ag^{+}, Fe^{2+}, Pt^{2+}, Zn^{2+} and Pb^{2+} [42,43]. However, evidence of the removal efficiency measured through the decrease in toxicity to *in vivo* biological models, such as fish, remains scarce. Thus, in this study, we used the model species zebrafish in its embryonic form to assess the potential of CDs as a multipurpose system for *in vivo* real-time detection and passivation of metallic ions. Therefore, three metal ions were selected: Cd^{2+}, Ni^{2+}, and Ag^{+}. The ability of the CDs to detect the ions and mitigate their toxicity was evaluated using fluorescence microscopy and toxicity assays, respectively. These metallic ions were selected because of their well-known high environmental hazards. Indeed, these metals have important anthropogenic uses with diverse entry routes in the aquatic environment including mining/smelting runoff, industrial effluents and atmospheric deposition in the case of Cd^{2+} and Ni^{2+} (Wright and Welbourn, 1994)' (Begum et al., 2022) and industrial discharges related to electronics manufacturing and runoff from consumer products containing silver or silver nanoparticles (e.g. washing of silver-treated textiles) (Padhye et al., 2023; Ding et al., 2019). Additionally, Ag^{+} is increasingly utilized in aquaculture to effectively control a wide range of pathogens, including bacteria, fungi, and viruses, thereby improving water quality and reducing the incidence of disease outbreaks. Recent advances have explored the use of silver nanoparticles to enhance efficacy (Khursheed et al., 2023). However, the use of Ag^{+} presents some risks, including its potential toxicity to aquatic organisms and bioaccumulation, which can impact both animal health and food safety (Li et al., 2023; Kakakhel et al., 2021).

Zebrafish embryos were chosen because they are a biological model widely used in ecotoxicology, with a battery of available endpoints that can be analyzed to assess the effects and modes of action of compounds, including lethal, morphological, behavioral, biochemical, and molecular parameters (Dai et al., 2014). Moreover, embryonic forms until free feeding (up to 5 days post fertilization in the case of zebrafish) are, according to the European directive 2010/63/EU on the protection of animals used for scientific purposes, considered alternative experimental models and their use promoted to the detriment of adult organisms.

Although previous studies have demonstrated that CDs are highly effective for the selective detection of several metals in aqueous solutions, to the best of our knowledge, this study is the first to demonstrate the effectiveness of CDs in mitigating metal toxicity (Ni^{2+}, Cd^{2+}, and Ag^{+}) using the zebrafish embryo model, resulting in a significant reduction of toxicity (Umar et al., 2023; Huang et al., 2018; Liu et al., 2020; Chung et al., 2021; Bai and Tang, 2023; Zhou et al., 2023; Zhu

et al., 2022). Furthermore, we highlight the capability of CDs for *in vivo* fluorescence-based metal contamination sensing.

2. Material and methods

2.1. Synthesis of CDs

The CDs were synthetized as previously reported (Mauro et al., 2022a). The precursors used were urea, citric acid, and indocyanine green (IGC). The solvothermal reaction was conducted in anhydrous N, N-dimethylformamide (DMF) (100 mL) at 170 °C for 6h in a still autoclave (Büchi AG, Miniclave Steel Type 3, Gschwaderstrasse, Switzerland). The work-up consisted of removal of the solvent under vacuum (25 mbar, 80 °C), redispersion of the crude slurry in water (150 mL), and purification by gel permeation chromatography (GPC) using Sephadex G10, G15, and G25 as the stationary phase. Among the collected fractions, the most fluorescent and homogeneous was selected for comprehensive physicochemical and biological characterizations (Mauro et al., 2022a).

2.2. Characterization of the CDs

Fourier transform infrared (FTIR) spectroscopy was used to assess the surface functional groups of the CDs. Measurements were performed using a PerkinElmer Spectrum Two IR spectrometer (Waltham, MA, USA), and the spectra were recorded in the range of 4000–400 cm^{-1}. The samples were prepared in dried KBr dishes. The chemical composition was also studied by ^{1}H NMR spectroscopy in a D_2O dispersion using a Bruker Avance II 300 spectrometer operating at 300.12 MHz.

The size distribution of the CDs was assessed via atomic force microscopy (AFM) using a Bruker FAST-SCAN microscope equipped with a closed-loop scanner. Scans were recorded in soft tapping mode using a FAST-SCAN-A probe with an apical radius of 5 nm. The sample was prepared by depositing 10 μL of an aqueous dispersion (0.1 mg mL^{-1}) on a mica dish and dried under vacuum (10 mbar) before analysis. The average diameter of the CDs was extrapolated from the AFM micrographs based on their height.

The CDs were structurally characterized using high-resolution transmission electron microscopy (HRTEM). The HRTEM measurements were carried out on an aberration-corrected FEI Titan3 80–300 microscope operating at an electron energy of 300 keV. Samples were prepared at room temperature in air by the deposition of a drop of an aqueous dispersion of CDs (0.2 mg mL^{-1}) on a commercial 400 μm mesh Cu grid (Plano 01824) covered by a holey amorphous carbon film with a nominal thickness of 3 nm. HRTEM images were evaluated by calculating the two-dimensional Fourier transform (FT), which yields information on the crystal structure (lattice parameters and crystal symmetry) of the individual nanoparticles. The analysis was performed by comparing the experimental FT with calculated diffraction patterns with Miller indices.

2.3. Ecotoxicological assessment

2.3.1. Testing compounds

Cadmium chloride hemypentahydrate (CAS Number: 7790-78-5), nickel sulfate hexahydrate (CAS Number: 10101-97-0), and silver chloride (CAS Number:7783-90-6) obtained from Sigma Aldrich were used as the sources of Cd^{2+}, Ni^{2+}, and Ag^{+}, respectively. All metals used were water-soluble at the tested concentrations; thus, stock solutions were prepared by directly dissolving the salts in the zebrafish system water.

2.3.2. Test organisms

Zebrafish were maintained in a Zebtec (Tecniplast) recirculating system at the Department of Biology of the University of Aveiro. Fish were maintained at a temperature of 27 ± 1 °C, 12:12 h light/dark photoperiod cycle, conductivity of 750 ± 50 μS/cm, and dissolved oxygen above 95 %. All fish were fed daily with Gemma Micro 500 (Skretting, Spain). To obtain zebrafish eggs, 12 fish (six males and six females) were placed in breeding tanks (Tecniplast) on the previous day. A divider was used in the aquarium to separate the males and females. On the test day, the divider was removed at the onset of illumination and the fish were allowed to breed. The eggs were then removed, rinsed in water, and selected under a stereomicroscope (Nikon Model SMZ1500 Stereomicroscope). Embryos at the blastula stage were selected for assays.

2.3.3. Preliminary assays

To establish the concentrations of metals to be tested in combination with the CDs, an assay was deployed for each metal (alone) following the OECD guideline 236 - Fish Embryo Toxicity (FET) (OECD, 2013). The objective was to select a concentration range from 0 to 100 % mortality so that LC_{50} (lethal concentration for 50 % of the exposed individuals) values could be computed. Embryos (24 per concentration) were individually placed in the wells of a 24-well plate containing 2 mL of the test solution in a randomized plate design. Test solutions were obtained by the successive dilution of a stock solution prepared by directly dissolving the metal salt in fish water. Testing conditions of temperature, photoperiod, conductivity, pH, and oxygen were as described for the fish culture. Embryonic mortality was observed daily using a stereomicroscope.

2.3.4. Combined exposure of metals and CDs

Based on preliminary tests, the following ranges of concentrations were selected for Cd^{2+}: 0, 19.3, 28.9, 43.4, 64.8, 145.8, 219.0 and 328.4 μM to assess lethal effects and 0, 0.2, 0.3, 0.5 and 0.7 μM to assess sublethal effects. For Ni^{2+} 0, 70.8, 98.9, 138.5, 194.0, 271.6 and 380.4 μM were used to assess lethal effects; 0, 84.8, 118.8, 166.4 and 232.9 μM to assess AChE activity and 0, 18.6, 26.0, 36.4, 51.0 and 71.4 μM were used to assess behavioural endpoints. For Ag^{+} 0, 0.1, 0.2, 0.4, 0.8 and 1.5 μM were used for the lethal effects and 0, 0.02, 0.04, 0.07, 0.14, 0.30 and 0.56 μM to assess locomotor activity and AChE activity. Zebrafish embryos were exposed to each metal concentration and each of the three CDs conditions (0, 5, or 50 mg mL^{-1}) following a full factorial design. Embryos (24 per treatment) were placed individually in 24-well plates with 2 ml of the test solution in a randomized plate design, and test solutions were obtained by successive dilution of the stock solution in zebrafish water enriched with the respective concentrations of CDs. The testing conditions (temperature, photoperiod, conductivity, pH, and oxygen) were similar to those described for the fish culture. Daily observations were made over 96 h under a stereomicroscope to record mortality, hatching, and malformations of the embryos. After 144 h of exposure, the movement of zebrafish larvae was studied using the ZebraBox video tracking system (software version 3.22, Viewpoint Life Sciences, Lyon, France). The equipment consisted of a 25 fps (frames per second) digital infrared video camera enclosed in a light-tight hood. As 120h zebrafish larvae tend to have a very low baseline locomotor activity in the light, the sudden change from light to dark conditions is used as a startle to induce locomotion in the organisms. The movement of the larvae was recorded for 2 min in the dark after an acclimation period of 6 min in light. The parameters recorded included the distance travelled by the larvae (swimming distance) and the swimming pattern (path angle). The path angles were evaluated by establishing four classes of angles, as described by Zhang et al. (2017) (Class 1 includes path angles between 90 and 180° which indicate zig zag or erratic movements; Class 2 includes angles between 30 ° and 90°; Class 3 includes angles between 10 ° and 30°, and Class 4 includes angles between 0 ° and 10°, which indicate straight movements, see Fig. S1).

At the end of the test, surviving larvae were sampled to determine AChE activity, and pools of five larvae were placed in a 2-ml microtube and frozen at −80 °C until analysis. A minimum of five pools (replicates) were used for each condition. The determination was performed

following the spectrophotometric method described by Gravato et al. (2021) The activity was expressed in nanomoles per milligram of protein. Protein concentration was determined at 595 nm using globulin as a standard, according to the Bradford method (Bradford, 1976). A Multiskan FC Microplate Photometer was used for analysis.

2.4. Photophysical characterization of the CDs

UV–vis absorption spectra were recorded using a JASCO V-540 spectrophotometer. The photoluminescence spectra were recorded using a Horiba Jobin Yvon Fluorolog 3–22 spectrofluorometer equipped with a 450 W xenon lamp. The photophysical characterization of the CDs was performed in water using 0.5 cm path length quartz cells. Titrations were carried out by the addition of microliters of the metal solutions (Cd^{2+}, Ni^{2+}, and Ag^{+}) and the CDs in zebrafish culture water using a 0.5 cm path length of cells. All measurements were performed at 298 K.

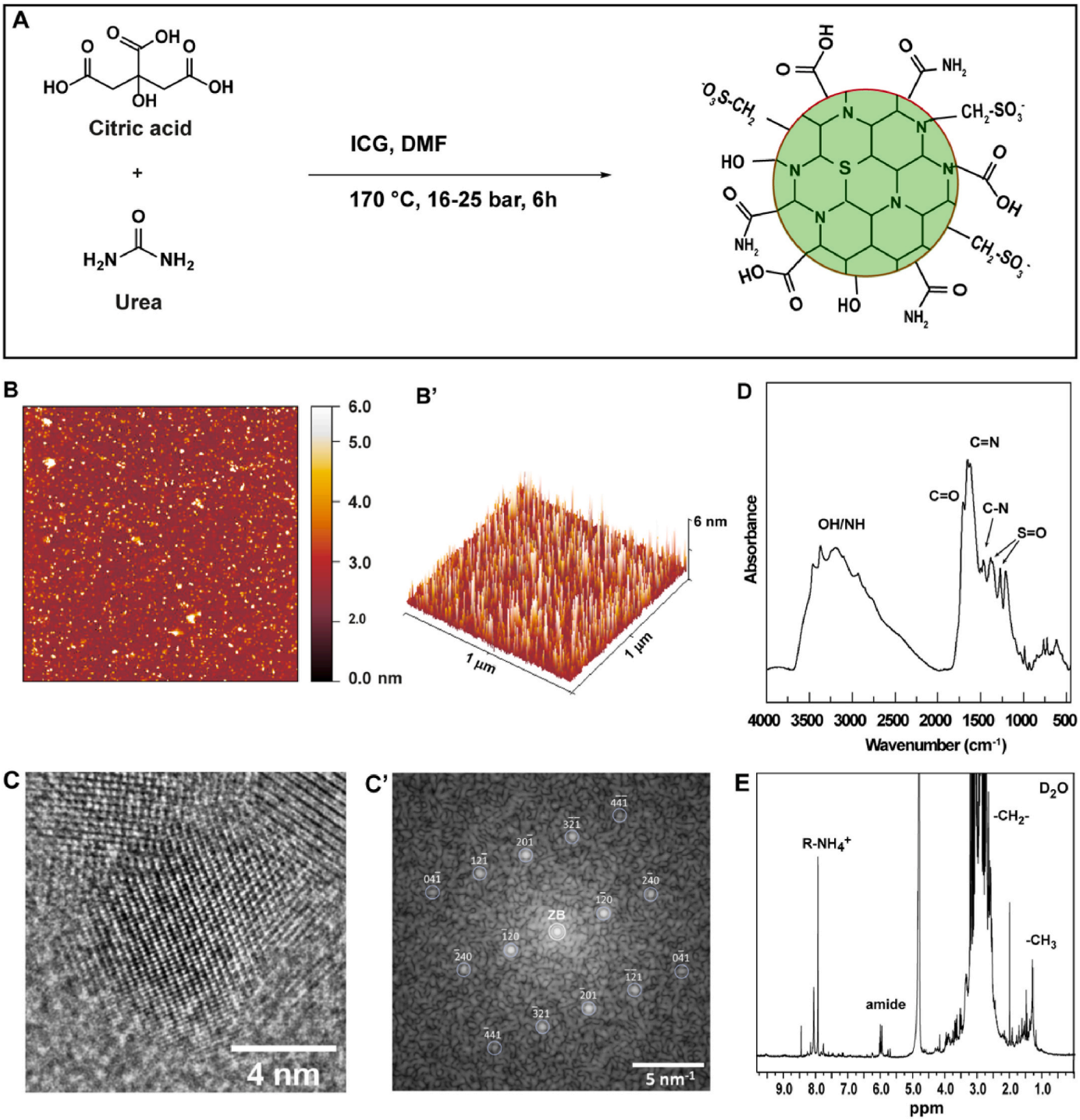

Fig. 1. – Synthetic pathway adopted for the synthesis of CDs (A). Atomic force microscopy (AFM) images of CDs (B-B′). HRTEM micrograph of a single, monocrystalline CD (C) and its FT with calculated diffraction pattern with Miller indices of bulk hexagonal β-C3N4 in the [214]-zone axis (C′). The zero-order beam (ZB) is indicated by a white circle. (C′). FTIR spectrum of CDs in KBr (D). ^{1}H NMR spectrum of CDs in D_2O (pD = 5.4) (E).

2.5. Imaging of the zebrafish larvae

A study of zebrafish fluorescence after exposure to CDs and metals was performed to confirm the data obtained from the photophysical assessment. Zebrafish embryos were subjected to 138.5 μM Ni^{2+}, 0.2 μM Ag^{+}, or a control in combination with 0 or 50 mg mL^{-1} CDs, following the experimental design described in Section 2.2. At the end of the exposure period, the larvae were washed in zebrafish culture water to remove CDs and frozen until observation (up to 2 days later). Imaging of the zebrafish embryos was carried out using a ZEISS Axio Imager 2 (Carl Zeiss, Germany) and ZEISS ZEN Blue software. The bright field and fluorescence images of zebrafish larvae were acquired using a 5× objective and processed using the Fiji Image J software.

2.6. Statistical analysis

The LC_{50} and EC_{50} values of the metals under different CDs conditions were calculated by adjusting a four-parameter logistic model to survival or hatching data. Various statistical models were employed to investigate the effects of metal concentration, CD treatment, and their interaction on zebrafish larvae. Generalized Linear Models (GLM) with a binomial distribution and logit link function were used to analyze the survival and hatching data. Swimming distance and AChE activity data were analyzed using Linear Models (LM). The effects on the proportion of locomotion angles were examined through Multinomial Logistic Regression Models using the R package "nnet" (Venables and Ripley, 2002). The validity of all the models was confirmed through residual diagnostics. All statistical analyses were performed using R v4.0.0 (R Core Team. R core team, 2021)' (Venables and Ripley, 2002).

3. Results

3.1. Synthesis and characterization of CDs

The solvothermal decomposition of citric acid, urea and sulfur doping agents such as ICG in DMF yields nitrogen-sulfur-doped CDs (Fig. 1A) endowed with multicolor emission and stable colloidal stability in aqueous dispersion due to the presence of surface polar groups (Mauro et al., 2022b, 2023). To obtain CDs with a high reaction yield and homogeneous size distribution, the sample was purified by column size-exclusion chromatography using water as the mobile phase. After purification, a dark powder with high reaction yields was obtained for the CDs (45 % w w^{-1}).

The AFM micrographs presented in Fig. 1B–B' show homogeneous ultrasmall nanoparticles of 5.4 nm in diameter with a minimal propensity for aggregation during the drying process. This can be ascribed to the polar groups that are usually present on the surface of the CDs. The crystalline nature of the carbonaceous core of the CDs was studied by HRTEM analysis, which revealed that the CDs have a β-C_3N_4 lattice with a hexagonal structure (Fig. 1C–C'). The size, morphology, and crystalline nature of the carbonaceous core of the CDs were studied using HRTEM. The size distribution of the CDs was dm = 5.3 ± 1.2 nm, as determined by the statistical evaluation of >200 CDs in several HRTEM images (Fig. S2). The structure of single, monocrystalline CD cores, such as that shown in the HRTEM image in Fig. 1C, was determined by calculating its 2-dimensional FT, which agreed with the calculated diffraction pattern with Miller indices of bulk hexagonal β-C_3N_4 (P63/m, group no. 176, lattice parameters of a = b = 6.38 Å, c = 2.395 Å) in the [214]-zone axis (Fig. 1C').

FTIR spectrum confirmed the polar nature of the CDs surface (Fig. 1 D), showing characteristic vibrations of hydroxyl (nO-H, 3420 cm^{-1}), amine (nN-H, 3200 cm^{-1}), carboxyl (nC=OOH, 1719 cm^{-1}), amide (nC=ONH, 1640 cm^{-1}; in plane dC=ONH, 1520 cm^{-1}), and sulfonate (nasS=O, 1180 cm^{-1}; nsS=O, 1050 cm^{-1}; nC-S, 995 cm^{-1}) groups. Furthermore, ^{1}H NMR spectroscopy showed that the CDs surface consisted of polar structures, mainly derived from the partial decomposition of the starting monomers (Fig. 1 E). In particular, there are groups of resonances at 1.4–1.6 ppm which can be ascribed to CH_3 residues of the citric acid moieties. The aliphatic CH_2 groups can be distinguished at 3.3–2.8 ppm. There are also characteristic peaks of primary amide (upfield) and secondary amide/primary amines (downfield) at 6.0 and approximately 8.0 ppm, respectively.

The absorption spectrum of the CDs in aqueous solution shows a strong band in the UV region, that is usually attributed to the n–π* transition of the C=O band and π–π* transition of the C=C band (Mohammad-Jafarieh et al., 2021) (Fig. 2). Furthermore, the prominent peak at 350 nm can be ascribed to the large number of amide bonds attached to the surface of the carbon core, undergoing an n - π* transition (Hess et al., 2017). In addition, small absorption bands were detected at 490 and 560 nm, which were assigned to the C=N absorption of pyridinic-N and pyrrolic-N, respectively. However, it is important to note that the chemical complexity of the CD surface makes it difficult to directly correlate specific absorption features with individual surface moieties. Considering that the surface is composed of amide, carboxyl, hydroxyl, and SOx groups, it is reasonable to attribute these transitions to multiple functions. Moreover, previous studies on S-doped CDs have demonstrated similar effects (Yang et al., 2019).

Exciting the solution at 300 nm produced a dual-band emission, as shown in Fig. 2. The band displayed a complex structure characterized by two peaks at 448 and 547 nm, suggesting the presence of two different chromophores simultaneously excited at the same energy. This behaviour is typical of CDs derived from citric acid and urea (Gazzetto et al., 2020). CDs exhibited excitation-dependent emission, with the emission peak progressively red-shifting as the excitation wavelength increased (Fig. S3). A maximum quantum yield (QY) of 6 % was observed in the green region (Mauro et al., 2022a). This characteristic is typically associated with structural and compositional heterogeneity, including differences in the size of the sp^2-conjugated domains and the nature of the surface functional groups (Santos et al., 2018).

3.2. Combined toxic effects of Cd^{2+} and CDs to zebrafish embryos

As expected, the survival of zebrafish embryos was significantly reduced by Cd^{2+} exposure (Table S1). LC_{50} values obtained for Cd^{2+} alone at 48 h were 56 ± 4; 147 ± 4 and 110 ± 6 μM for CDs concentrations of 0.0, 5.0 and 50.0 mg L^{-1} respectively. At 96 h post fertilization (hpf) these values were 49 ± 6; 143 ± 12 and 99 ± 4 × 10^6 μM for CDs concentrations of 0.0, 5.0 and 50.0 mg L^{-1} respectively. At both time points, LC_{50} values were at least twice lower for the treatment in which CDs were not used compared to the values calculated for the treatments in which CDs were employed. The increase in the LC_{50} values with the use of CDs can be graphically observed by the displacement of

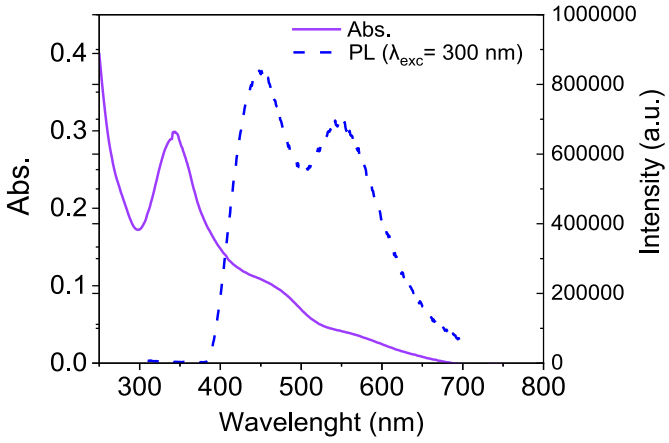

Fig. 2. UV–vis absorption and emission (dashed line, λ_{exc} = 300 nm) spectra of CDs in water.

the dose response curve to the right in the conditions of CDs = 5 and 50 mg L^{-1} (Fig. 3A and B). Statistical analysis confirmed the effects of CDs on the observed effects (Table S1). Embryo hatching was significantly depressed by Cd^{2+} (Table S1, Fig. 3 C). However, despite a statistically significant interaction between Cd^{2+} concentration and CDs treatment, the effects on the EC_{50} of the CDs were not evident after 72 h of exposure.

Moreover, the results showed that Cd^{2+} exposure inhibited the locomotor function of the larvae by reducing the swimming distance (Table S2, Fig. 3D). This effect did not change upon the addition of CDs. Regarding the measured path angles during larval movement, the results showed that Cd^{2+} exposure decreased the proportion of class 4 angles (straight movements) and increased the proportion of angles from the other classes, particularly class 1 (denoting erratic swimming). The addition of CDs clearly altered this effect, and no significant erratic behavior was observed. (Table S3, Fig. 3 E). Additionally, AChE activity was not affected by Cd^{2+} exposure or the addition of CDs (Table S2, Fig. 3 F).

3.3. Combined effects of Ni^{2+} and CDs to zebrafish embryos

Ni^{2+} exposure significantly reduced embryo survival (120 h: LC_{50}, 248 ± 7 μM). The use of CDs significantly reduced Ni^{2+}-induced mortality, as indicated by the increase in the LC_{50} value calculated for CDs =

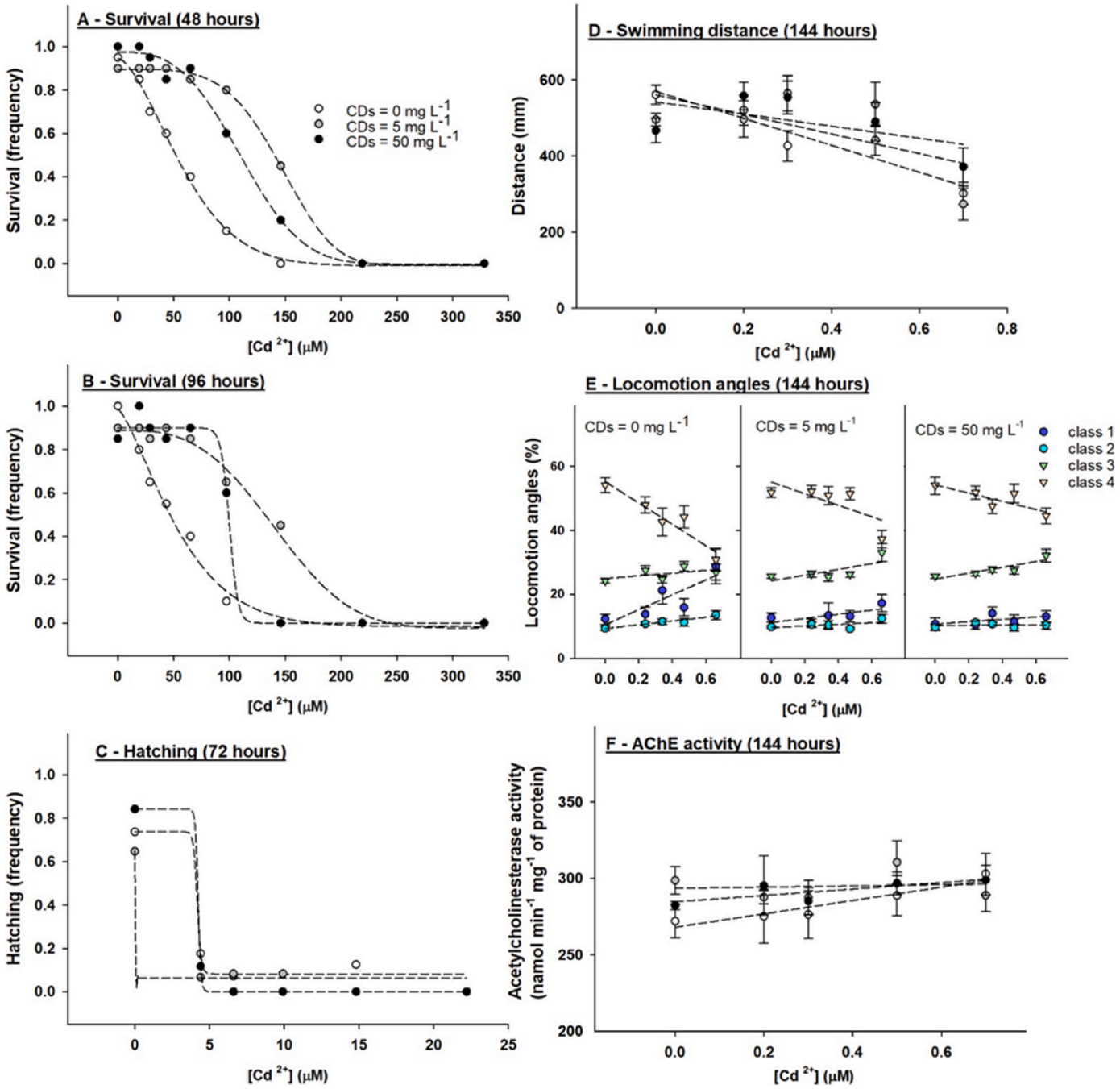

Fig. 3. Effects of Cd^{2+} in combination with different concentrations of carbon dots (CDs) on several parameters measured in zebrafish embryos. In A, B, and C, data are mean values, and slashed lines are 4-parameter logistic curves adjusted to the data. In D, E, and F, data are mean values ± standard error, and slashed lines are linear models adjusted to the data.

5 mg L^{-1}. For CDs = 50 mg L^{-1}, the low mortality levels did not allow for the calculation of the LC_{50}. In Fig. 4 A an increase in survival with increasing CDs treatments can be observed, particularly in the last Ni^{2+} concentration tested, where survival levels increased from 0 % at CD = 0 mg L^{-1} treatment to 50 % at CDs = 5 mg L^{-1} and to ~70 % at CD = 50 mg L^{-1} treatment (Table S4). Ni^{2+} exposure also suppressed embryo hatching (72 h, EC_{50} = 170 ± 40 μM) (Fig. 4 B). Concomitant exposure to CD (50 mg L-1) and Ni^{2+} counteracted the hatching inhibition observed with Ni^{2+} alone (EC_{50} = 190 ± 18 μM). However, CD = 5 mg L^{-1} was not sufficient to observe any change in Ni^{2+} effects (EC_{50} = 164 ± 15 μM). Ni^{2+} exposure increased the distance travelled by the larvae only in the no CDs treatment; this effect was nullified by the presence of CDs (Table S5, Fig. 4 C). The proportion of angles from the different classes seemed to change with Ni^{2+} exposure, namely, an increase in the proportion of class 4 angles and a decrease in the proportion of class 1 angles were observed, particularly at the highest concentrations tested. These effects were no longer visible in the presence of 5 and 50 mg L^{-1} of CDs (Table S6 and Fig. 4 E).

Similarly, the AChE activity slightly decreased with Ni^{2+} exposure, but this effect ceased with the addition of CDs (Table S5, Fig. 4 D).

3.4. Combined effects of Ag^{+} and CDs to zebrafish embryos

Ag^{+} was highly toxic to zebrafish embryos (Table S7). LC_{50} values obtained for Ag^{+} at 96 h were 0.4 ± 0.02 and 0.8 ± 0.3 μM for CDs = 0 and 5 mg L^{-1} respectively. For CDs = 50 mg L^{-1}, the LC_{50} could not be calculated because of data variability. In Fig. 5 A the increased survival rate in the CDs treatments can be observed, particularly at the concentration of 0.8 μM of Ag^{+} where survival levels increased from 20 % at CD = 0 mg L^{-1} treatment to 80 % at CDs = 5 mg L^{-1} and to 100 % at CD = 50 mg L^{-1} treatment. The hatching rate at 72 h did not seem to be affected by Ag^{+} exposure (Table S7, Fig. 5 B).

Exposure to Ag^{+} ions increased the distance travelled by larvae (Table S8, Fig. 5 C). Although statistical significance was found for the effects of the CDs, no clear effect was observed. Regarding locomotion path angles, Ag^{+} appeared to increase class 1 angles and decrease class 3 angles. The addition of CDs did not revert Ag^{+} effects but changed the response type; class 3 angles still decreased, but class 4 angles increased (Fig. 5 E). Larval AChE activity decreased with exposure to Ag^{+}; however, this effect was not observed at CDs = 50 mg L^{-1} (Fig. 5 D).

3.5. Photophysical characterization of CDs

The sensorial ability of the CDs to the metal ions Cd^{2+}, Ni^{2+}, and Ag^{+} was determined by titration with the addition of small amounts of metallic salts. Interestingly, the CDs exhibited distinct fluorescence behavior upon interaction with different metal ions. In studies with Ni^{2+}, a significant concentration-dependent reduction in the emission intensity was observed, with a high incidence in the band centered at 550 nm (Fig. 6 A). The increase in the concentration of Ni^{2+} from 9.3 μM up to 84.1 μM (LC_{50} value for zebra fish survival) showed a significant decrease of emission intensity (Fig. 6 B). In the case of Cd^{2+}, strong quenching of the emission intensity was preferentially observed for the band centered at 450 nm in a concentration-dependent manner (Fig. 6 A). A significant decrease in fluorescence intensity is detected from starting concentrations of 3.7 μM–33.5 μM (LC_{50} value for zebra fish survival) of Cd^{2+}. Finally, the interaction of the CDs with the Ag^{+} ions enhanced the photoluminescence of the CDs (Fig. 6 A). A higher contribution was observed for the band centered at 550 nm, which was dependent of the concentration of Ag^{+} ions, ranging from 0.1 μM up to 0.8 μM (Fig. 6 B). Notably, no significant shift in the emission maximum was observed. The different quenching of emission as a function of the metal ions in solution demonstrates that the two peaks stem from two different electronic transitions that interact differently with the ions.

3.6. Fluorescence imaging of zebrafish embryos exposed to CDs and metals

To investigate the fluorescence behavior of the CDs and the increment or quenching of the fluorescence in the presence of metals within zebrafish larvae, images were recorded in both bright field and fluorescence modes. Fig. S4 shows a comparative analysis between control zebrafish larvae and those kept in a medium containing 50 mg L^{-1} of CDs, showing very low fluorescence levels in the control embryos compared to the CD-exposed organisms. In addition, Fig. 6C shows the fluorescence of the larvae exposed to various conditions; the fluorescence of the CDs was reduced in the presence of Ni^{2+} and increased in the presence of Ag^{+}. This pattern was also observed in the total fluorescence intensity measured (Table S10).

4. Discussion

CDs with multicolor bright emissions were synthesized with exceptionally high reaction yields (45 %) and remarkable size homogeneity (5.3 ± 0.3 nm). The exceptionally high reaction yield observed enables bulk applications that are often precluded by many synthetic protocols relying on yields of only 1–5 % (Mauro et al., 2022c). These CDs feature hydroxyl, amine, sulfonate, and carboxylic acid groups on their surfaces, enabling diverse interactions with a wide range of ions under dynamic conditions. Polar CDs can detect monovalent and divalent ions through fluorescence changes, making them highly promising for monitoring pollutants in solutions. In addition, these CDs contain sulfonate and carboxylic acid groups, which are expected to be highly effective for complexing heavy metal ions, with significant effects on their fluorescence properties. However, to the best of our knowledge, no study has investigated the efficiency of CDs in mitigating the acute effects of Cd^{2+}, Ni^{2+}, and Ag^{+} during the early life stages of zebrafish.

Metals share a common mechanism of acute toxicity in zebrafish. Alsop and Wood (2011) demonstrated that several metals, including Cd^{2+} and Ni^{2+} decreased Ca^{2+} uptake, although metal toxicity was attributed to whole-body ion loss (predominantly Na^{+}). The toxic effects of Cd^{2+} on zebrafish embryos are well described in the literature and are mediated by oxidative stress, mitochondrial dysfunction, endocrine disruption, and interference with the cholinergic system (Morrice et al., 2018; Frasco et al., 2005; Park et al., 2020). This leads to a range of effects including hatching delay, locomotor dysfunction, and increased mortality rates (Aldavood et al., 2020), as observed in the present study. A 48 h LC_{50} value of 168 μM was obtained, which was in the same range as that obtained by Hallare et al. (2005) who also observed a concentration-dependent decrease in hatching rate. As mentioned earlier, Cd^{2+} further interfered with the locomotion function of zebrafish larvae, decreasing the distance travelled by organisms and changing the proportion of different classes of angles measured during locomotion. Decreased swimming distance or hypoactivity of zebrafish larvae after Cd^{2+} exposure has already been documented in studies by Xu et al. (2022), which suggested interference of the metal with the startle response or reactivity of the larvae. In contrast, in the present study, the proportion of class 4 angles (indicative of ordinary straightforward movement) decreased, while class 1 angles (indicative of movement with great changes in direction) increased with Cd^{2+} exposure, suggesting an erratic movement pattern, which is a sign of anxiety in fish. Xu et al. (Frasco et al., 2005) observed a significant increase in the turn angles which is likely related to the swimming pattern change observed in this study. Locomotion parameters are usually regarded as relevant from an ecological perspective given that locomotion impairments can be easily linked to important ecological functions such as predator avoidance, feeding behavior, reproduction, and interaction with conspecifics (Scott and Sloman, 2004).

The addition of CDs reduced the intensity of these effects in terms of the mortality rate and erratic swimming, clearly demonstrating the effectiveness of CDs in mitigating Cd^{2+} toxicity. In fact, the 48 h – LC_{50}

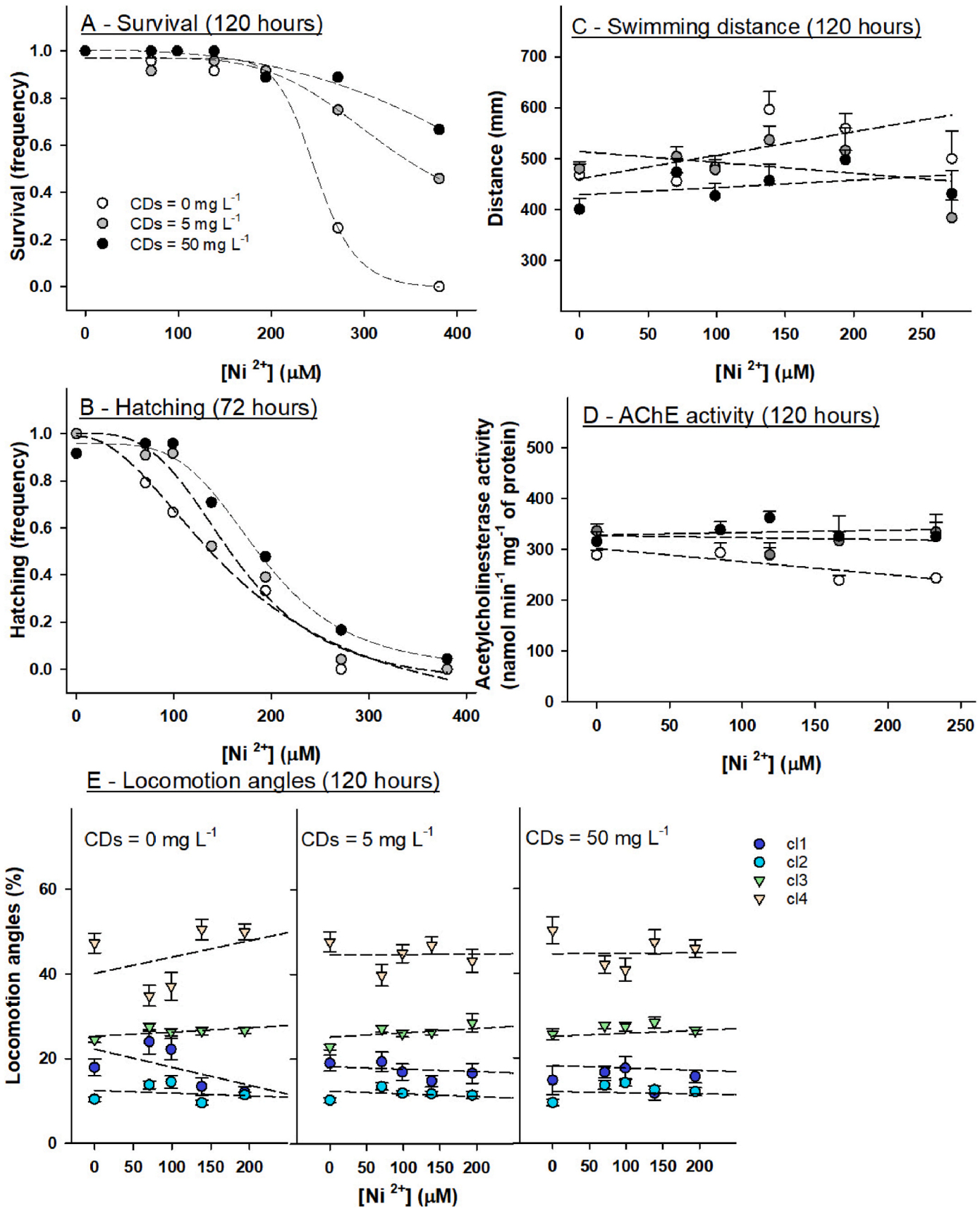

Fig. 4. Effects of Ni^{2+} in combination with different concentrations of carbon dots (CDs) on several parameters measured in zebrafish embryos. In A and B, data are mean values, and slashed lines are 4-parameter logistic curves adjusted to the data. In C, D, and E, data are mean values ± standard error, and slashed lines are linear models adjusted to the data.

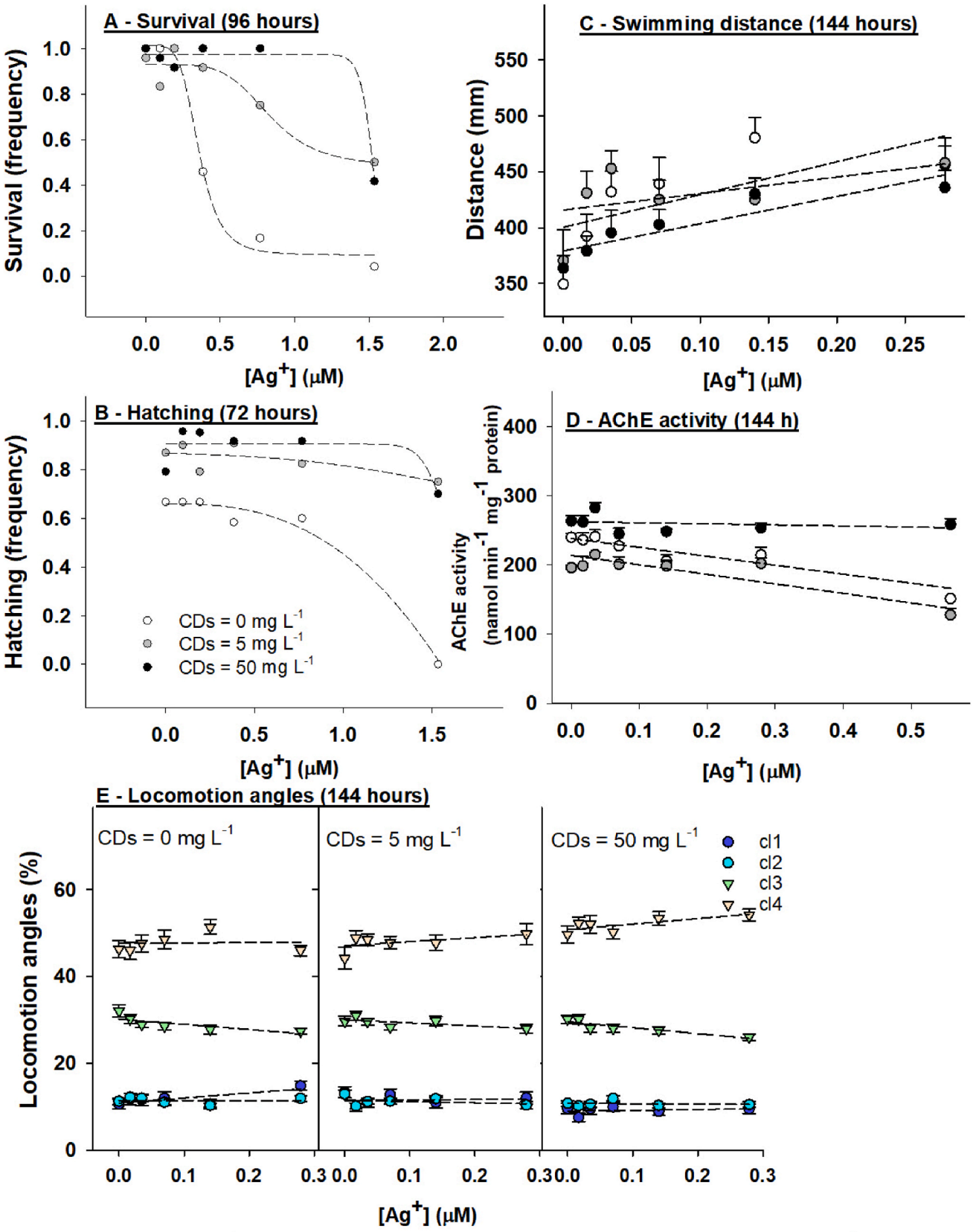

Fig. 5. Effects of Ag^{+} in combination with different concentrations of carbon dots (CDs) on several parameters measured in zebrafish embryos. In A and B, data are mean values, and slashed lines are 4-parameter logistic curves adjusted to the data. In C, D, and E, data are mean values ± standard error, and slashed lines are linear models adjusted to the data.

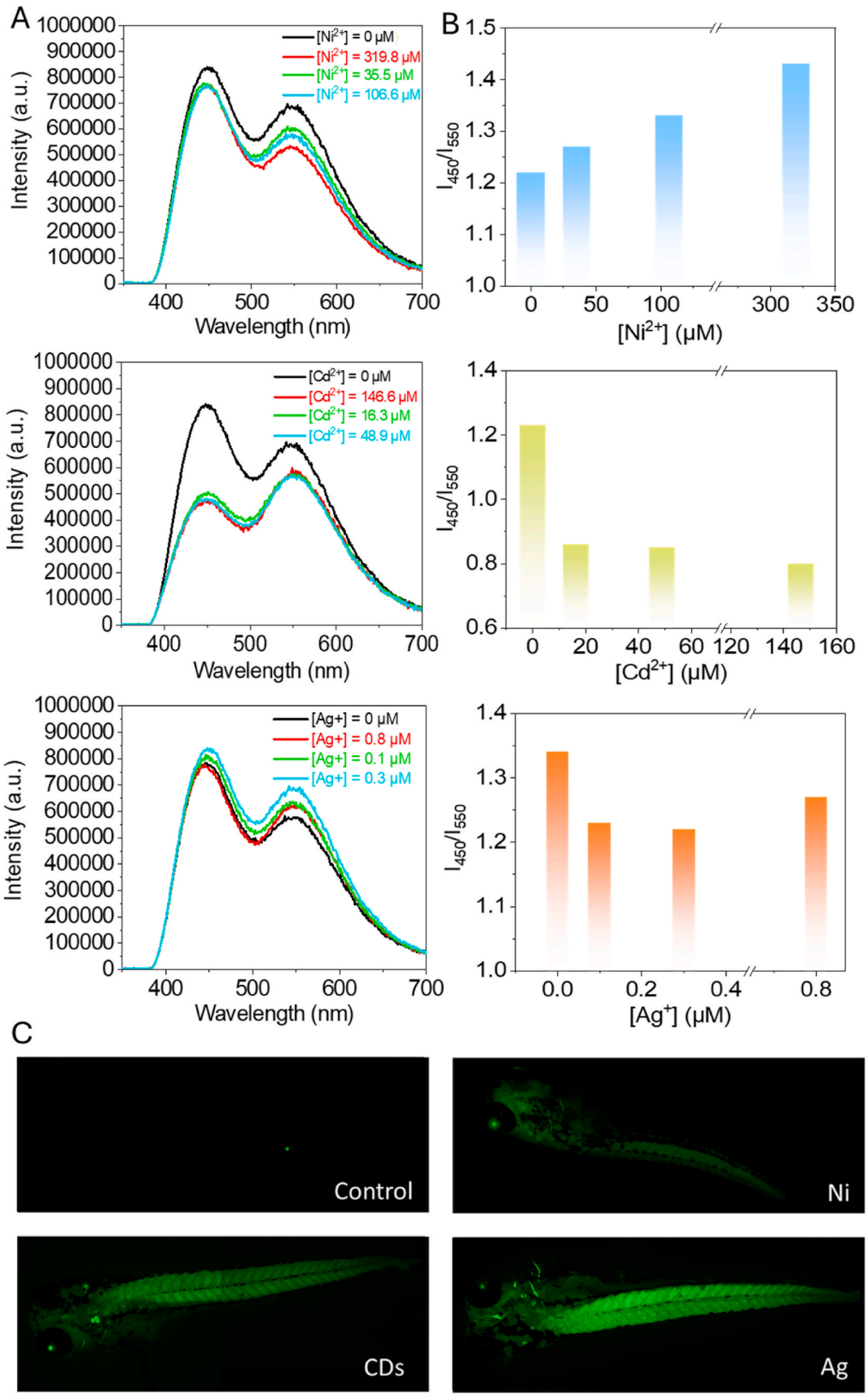

Fig. 6. A) Titration data for CDs (5 mg L^{-1}) in water upon successive addition of Ag^{+}, Ni^{2+}, and Cd^{2+} –emission spectra recorded at $\lambda_{exc} = 300$ nm. B) Fluorescence emission ratio (I_{450}/I_{550}) before and after addition of the relevant analytes at different concentrations. C) Fluorescence images of control zebrafish (upper left), CDs only (bottom left), CDs + 319.8 µM of Ni^{2+} (upper right), and CDs + 0.8 µM Ag^{+} (bottom right).

increased from 56 to 110 μM with the addition of 50 mg L^{-1} CDs, while class 1 angles (indicative of erratic swimming) increased to 30 % after the exposure to 0.7 μM Cd^{2+} without CDs and remained at the initial levels (10 %) in the 50 mg L^{-1} of CDs treatment.

The reduction of the Cd^{2+} effect is likely to occur because of the capacity of the CDs to absorb a significant percentage of ions, thereby reducing the amount taken up by the embryos over the course of exposure. Previous studies have documented the adsorption of Cd^{2+} by CDs in aqueous solution. For example, Sabet et al. reported a CDs removal efficiency of 37 %, and Rahmani et al. reported an adsorption capacity of 12.60 mg g^{-1} (Sabet and Mahdavi, 2019b)' (Rahmanian et al., 2018). However, to the best of our knowledge, the only study that reported the mitigation of Cd^{2+} using living organisms (*in vivo* studies) was by Chen et al., who showed that nitrogen-doped CDs (N-CDs) alleviated plant stress in *Arabidopsis thaliana* in an aquatic environment by adsorbing Cd^{2+} ions (Chen et al., 2020).

With respect to Ni^{2+} exposure, a toxicity profile was obtained including a dose response curve for survival with a 120 h - LC_{50} = 148.2 μM and hatching with a 72 h - EC_{50} = 167 μM in agreement with the described by Aldavood et al. (2020) and Alsop and Wood (2011). Regarding locomotion, Ni^{2+} did not affect locomotion when assessed through swimming distance travelled by larvae but led to a change in the proportion of path angles from different classes (increment in linear movements and decrease in movements with changes in direction). The effects of Ni^{2+} on zebrafish locomotor behavior are expected, although they have not been well documented in the literature. For instance, Nabinger et al. (2018) observed for a similar exposure design an increase in the distance travelled by larvae and mean speed at concentrations of ~21 and 63 μM while for lower concentrations (~0.1 μM) a decrease in these parameters was observed. The authors also observed an increase in the absolute turn angle at 63 μM. In contrast, other authors, using a different experimental design (5 days old larvae acutely exposed to Ni^{2+} for 2 h), observed a decreased locomotor activity at concentrations between 128 and 255 μM (Kienle et al., 2009). These studies, including the present one, suggest some impairment in locomotor function after Ni^{2+} exposure. Moreover, nickel is not a typical cholinesterase inhibitor, as reported in the literature [e.g. 69], and observed in this study. Thus, a better characterization of the behavioral responses and mechanisms of action is needed.

CDs co-exposure with Ni^{2+} reversed the metal effects to different extents, depending on the parameters evaluated. Mortality was reduced to such a degree that the LC_{50} value could not be calculated for the CDs = 50 mg L^{-1} treatment (at the highest concentration tested, survival increased from 0 % at CDs = 0 mg L^{-1} to 50 and 70 % at CDs = 5 and 50 mg L^{-1}, respectively). The effects of CDs were also noticeable in the hatching rates (EC_{50} values increased from 167 to 190 μM at CDs = 0 and 50 mg L^{-1} respectively) and in the path angles where effects observed for Ni^{2+} alone were not detected in co-exposure with CDs 5 and 50 mg L^{-1}. This corroborates the results of Ajith et al. (2020b), who reported a removal efficiency of 79 % for Ni^{2+} ions by CDs obtained from the leaf extract of *Ficus benghalensis*.

Ag^{+} showed to be highly toxic to zebrafish embryos with a 96h - LC_{50} value of 0.4 μM, in the same order of magnitude as values previously described in studies such as Massarsky et al. (2013a) which reported a 96 h - LC_{50} of 0.6 μM. Hatching delay is another documented effect of Ag-ion exposure. For instance, Pereira et al. (2023) documented a 96 h - EC_{50} value of 0.18 μM of Ag^{+} to zebrafish embryos while Massarsky et al. (2013b) observed hatching delays at concentrations higher than 0.17 μM of Ag^{+} which were attributed to the underdevelopment of the larvae. However, in the present study, the effects on hatching were detected only at the highest concentration when the mortality levels were already very high. Ag^{+} toxicity is associated with osmotic disturbances arising from the suppression of gill Na^{+}/K^{+}-ATPase (Van Aerle et al., 2013a). Additionally, Ag^{+} ions exert cytotoxic effects by inactivating enzymes that bind to sulfhydryl groups, such as enzymes responsible for the regulating oxidative stress. Thus, reactive oxygen species (ROS) are generated after exposure to Ag^{+} ions (Van Aerle et al., 2013b).

Although there is no extensive research yet on the effects of Ag^{+} ions on swimming behavior-related parameters in zebrafish, a few reports can be mentioned, such as the work by Ašmonaitė et al. (Ašmonaite et al., 2016), who showed a noticeable reduction in the activity of the zebrafish larvae at Ag^{+} concentrations above 0.43 μM. In the present study, larval activity increased as well as the angles indicative of erratic swimming (class 1), which, along with the inhibition of AChE activity, may suggest a behavioral impairment mediated by disturbances in the cholinergic pathway. In fact, the inhibition of AChE activity, the enzyme responsible for recycling the neurotransmitter acetylcholine in the synaptic cleft, is usually associated with locomotor dysfunction. Vrèek and Sinko (Vrèek and Šinko, 2013) also reported decreased AChE activity after exposure to Ag^{+} ions *in vitro*, however *in vivo* studies are scarce.

After the combined exposure of zebrafish embryos to Ag^{+} and CDs, there was a significant increase in the LC_{50} values of larvae treated with CDs. Ag^{+} LC_{50} was 2 and 4 times higher in the embryos exposed to 5 and 50 mg L^{-1} of CDs respectively when compared to embryos not exposed to CDs, suggesting, similarly to the observed for Cd^{2+} and Ni^{2+} an important role of CDs in the reduction of the metal toxicity.

The addition of CDs did not revert the Ag^{+} effects at the behavioral level but changed the response type, suggesting their interference in the response the metallic ions. The decrease in AChE activity observed at CD = 0 was completely reversed at CDs = 50 mg L^{-1}. The endpoints of survival, hatching, and AChE activity strongly support the hypothesis that CDs mitigate Ag^{+} toxicity.

The sensorial ability of the CDs towards metal ions, determined by titration with the addition of small amounts of metallic salts, showed distinct fluorescence behavior for the interaction of CDs with different metallic ions, with a reduction in the emission intensity in the case of Ni^{2+} and Cd^{2+} ions and an increase in that of Ag^{+} ions. The reduction in fluorescence intensity in the presence of Cd^{2+}or Ni^{2+} ions as well as the enhancement observed with Ag^{+} ions (Fig. 6) were also confirmed by fluorescence microscopy. The fluorescence quenching of CDs has been widely reported in their interaction with several metal ions (XU et al., 2022). Cd^{2+}, classified as soft acid, and Ni^{2+}, a borderline Lewis acid, can coordinate with free oxygen and nitrogen atoms on the surface of CDs, promoting non-radiative pathways that result in emission quenching (Zu et al., 2017). In contrast, the fluorescence enhancement observed in the presence of Ag^{+} is typically attributed to the ability of surface functional groups on CDs to reduce Ag(I) to Ag (0), leading to the formation of silver nanoclusters that enhance the radiative emission of CDs (Jin et al., 2018; Gao et al., 2015). Moreover, metal-enhanced fluorescence of the CDs was observed when Ag^{+} was added to the initial CD solution, which might be ascribed to aggregation-induced emission enhancement. For example, Chen et al. reported a CDs single-peak emission enhancement dependent on Ag^{+} concentration, with a blue shift from 440 to 425 nm (Gao et al., 2015). Additionally, Jiao et al. reported ratiometric fluorescence emission with significant fluorescence varying from orange to green (Jiao et al., 2019). Nevertheless, the fluorescence enhancement effects are strongly dependent on the functional groups present in the CDs structure, as well as the respective optical features. Although significant research has explored CD fluorescence modulation through interactions with metallic ions, we demonstrated the potential of biomonitoring this effect in zebrafish. Fluorescence microscopy of embryos exposed to CDs and metals revealed their ability to detect specific metal contamination in zebrafish. This was evident through fluorescence quenching in the presence of Ni^{2+} ions and enhancement by Ag^{+} ions. These findings highlight the potential of CDs as selective biosensors for monitoring aquatic pollutants. Moreover, the interaction mechanisms described above reduce the bioavailability of metal ions within organisms, preventing them from reaching their molecular targets and thus either inhibiting typical metal toxicity effects or causing such effects only at higher concentrations.

5. Conclusions

In this study, the ability of CDs to significantly reduce Cd^{2+}, Ni^{2+}, and Ag^{+} lethal toxicity was demonstrated in a zebrafish embryo model highlighting their potential for environmental applications (Tran et al., 2023a; Nguyen et al., 2023; Hoang et al., 2025). However, the results for sublethal toxicity were inconsistent, with different endpoints supporting or not supporting the toxicity reduction by CDs depending on the metal studied. In the case of Cd^{2+}, survival at a concentration of 64.8 μM increased from 20 % in the treatment without CDs to 60 and 80 % in the treatments with 5 and 50 mg L^{-1} of CDs, respectively. The results also showed that CDs (50 mg L^{-1}) avoided the alterations observed in the swimming patterns, specifically the increment (from 10 to 30 %) of the angles indicative of erratic swimming (class 1) observed in the treatments without CDs. In the case of Ni^{2+}, survival at the highest concentration increased from 0 % in the treatment without CDs to 50 and 70 % in the treatments with 5 and 50 mg L^{-1} of CDs, respectively. Evidence of mitigation of the metal toxicity was also found for hatching where EC_{50} values of 167 and 190 μM were calculated for treatments without and with 50 mg L^{-1} CDs, respectively, and for swimming patterns. The swimming pattern changed upon Ni^{2+} exposure, with an increase from ~40 to ~50 % in class 4 angles and a decrease from 20 to 10 % in class 1 angles in the treatments where CDs were not used. When CDs were used, no alterations in the path angle proportions were observed. In the case of Ag^{+}, survival at concentration of 0.8 μM increased from 20 % in the treatment without CDs to 80 and 100 % in the treatments with 5 and 50 mg L^{-1} of CDs, respectively. CDs treatment at 50 mg L^{-1} also prevented the AChE inhibition observed after exposure to Ag^{+} alone. The CDs concentrations used (5 and 50 mg L^{-1}) seemed adequate to reduce metal toxicity; however, future studies should adjust these concentrations to achieve optimized efficiency.

Furthermore, we observed that CDs can be utilized to monitor specific ion contamination in water by fluorescence emission enhancement (Ag^{+}) or quenching (Ni^{2+} and Cd^{2+}). In addition, the fluorescence intensity ratio (I_{450}/I_{550}) provided a distinct fingerprint for each ion interaction. Importantly, *in vivo* fluorescence studies with zebrafish embryos demonstrated the ability of CDs to distinguish Ag^{+} contamination from Ni^{2+} and Cd^{2+}, although differentiation between Ni (Tang et al., 2021) and Cd^{2+} was not detectable.

A further understanding of the nature of CDs/metals interaction is needed for a possible scale up of this technology, including the long-term stability of the complexes and the behaviour of CDs in the presence of several metals in the aquatic environment.

CRediT authorship contribution statement

Inês Domingues: Writing – original draft, Resources, Conceptualization. **João Amaral:** Investigation. **Bruna Vieira:** Investigation. **Ana Luísa Machado:** Writing – review & editing, Formal analysis. **Carla I.M. Santos:** Investigation. **Joana P.M. Sousa:** Investigation. **Alice Sciortino:** Writing – review & editing. **Roberta Cillari:** Writing – review & editing. **Radian Popescu:** Writing – review & editing. **Yolita M. Eggeler:** Writing – review & editing. **Fabrizio Messina:** Writing – review & editing, Visualization, Resources. **Nicolò Mauro:** Writing – review & editing, Visualization, Resources. **Gil Gonçalves:** Writing – original draft, Visualization, Supervision, Conceptualization.

Declaration of competing interest

The authors declare that they have no known competing financial interests or personal relationships that could have appeared to influence the work reported in this paper.

Acknowledgments

This work was funded by national funds through FCT – Fundação para a Ciência e a Tecnologia I.P., under the project/grant UID/50006 + LA/P/0094/2020 (doi.org/10.54499/LA/P/0094/2020) – CESAM and UID 00481 Centre for Mechanical Technology and Automation (TEMA). We also acknowledge FCT financial support to the project CarboNCT - 2022.03596. PTDC (DOI 10.54499/2022.03596. PTDC, https://doi.org/10.54499/2022.03596.PTDC). R.C. thanks Fondazione Umberto Veronesi for the support by the FUV 2025 Fellowship

Appendix A. Supplementary data

Supplementary data to this article can be found online at https://doi.org/10.1016/j.envres.2025.122851.

Data availability

Data will be made available on request.

References

Ajith, M.P., Priyadarshini, E., Rajamani, P., 2020a. Effective and selective removal of heavy metals from industrial effluents using sustainable Si–CD conjugate based column chromatography. Bioresour. Technol. 314, 123786.
Ajith, M.P., Priyadarshini, E., Rajamani, P., 2020b. Effective and selective removal of heavy metals from industrial effluents using sustainable Si–CD conjugate based column chromatography. Bioresour. Technol. 314.
Ajith, M.P., Pardhiya, S., Rajamani, P., 2022. Carbon dots: an excellent fluorescent probe for contaminant sensing and remediation. Small 18, 1–27.
Aldavood, S.J., et al., 2020. Effect of cadmium and nickel exposure on early development in zebrafish (Danio rerio) embryos. Water (Switzerland) 12.
Alsop, D., Wood, C.M., 2011. Metal uptake and acute toxicity in zebrafish : common mechanisms across multiple metals. Aquat. Toxicol. 105, 385–393.
Arcudi, F., Đorđević, L., 2023. Supramolecular chemistry of carbon-based dots offers widespread opportunities. Small 19. https://doi.org/10.1002/smll.202300906. Preprint at.
Ašmonaite, G., Boyer, S., de Souza, K.B., Wassmur, B., Sturve, J., 2016. Behavioural toxicity assessment of silver ions and nanoparticles on zebrafish using a locomotion profiling approach. Aquat. Toxicol. 173, 143–153.
Bai, C., Tang, M., 2023. Progress on the toxicity of quantum dots to model organism-zebrafish. J. Appl. Toxicol. 43. https://doi.org/10.1002/jat.4333. Preprint at.
Begum, W., et al., 2022. A Comprehensive Review on the Sources, Essentiality and Toxicological Profile of Nickel. https://doi.org/10.1039/d2ra00378c.
Bhattacharjee, T., Konwar, A., Boruah, J.S., Chowdhury, D., Majumdar, G., 2023. A sustainable approach for heavy metal remediation from water using carbon dot based composites: a review. Journal of Hazardous Materials Advances 10, 100295.
Bradford, M.M., 1976. A rapid and sensitive method for the quantitation of microgram quantities of protein utilizing the principle of protein-dye binding. Anal. Biochem. 72, 248–254.
Bradl, H.B., 2005. Chapter 1 Sources and origins of heavy metals. Interface Science and Technology 6, 1–27.
Chen, Q., et al., 2020. Enhanced bioaccumulation efficiency and tolerance for Cd (II) in Arabidopsis thaliana by amphoteric nitrogen-doped carbon dots. Ecotoxicol. Environ. Saf. 190.
Chung, C.Y., et al., 2021. Toxic or not toxic, that is the carbon quantum dot's question: a comprehensive evaluation with zebrafish embryo, eleutheroembryo, and adult models. Polymers 13.
Dai, Y.J., et al., 2014. Zebrafish as a model system to study toxicology. Environ. Toxicol. Chem. 33, 11–17.
Ding, R., et al., 2019. Assessing the environmental occurrence and risk of nano-silver in Hunan, China using probabilistic material flow modeling. Sci. Total Environ. 658, 1249–1255.
Đorđević, L., Arcudi, F., Cacioppo, M., Prato, M., 2022. A multifunctional chemical toolbox to engineer carbon dots for biomedical and energy applications. Nat. Nanotechnol. 17. https://doi.org/10.1038/s41565-021-01051-7. Preprint at.
Ferraro, P.J., Prasse, C., 2021. Reimagining safe drinking water on the basis of twenty-first-century science. Nat. Sustain. 4 (12 4), 1032–1037, 2021.
Frasco, M.F., Fournier, D., Carvalho, F., Guilhermino, L., 2005. Do metals inhibit acetylcholinesterase (AChE)? Implementation of assay conditions for the use of AChE activity as a biomarker of metal toxicity. Biomarkers 10, 360–375.
Gao, X., et al., 2015. One-pot synthesis of carbon nanodots for fluorescence turn-on detection of Ag+ based on the Ag+-induced enhancement of fluorescence. J Mater Chem C Mater 3.
Gazzetto, M., et al., 2020. Photocycle of excitons in nitrogen-rich carbon nanodots: implications for photocatalysis and photovoltaics. ACS Appl. Nano Mater. 3, 6925–6934.
Gimeno-García, E., Andreu, V., Boluda, R., 1996. Heavy metals incidence in the application of inorganic fertilizers and pesticides to rice farming soils. Environ. Pollut. 92, 19–25.
Gravato, C., Abe, F.R., de Oliveira, D.P., Soares, A.M.V.M., Domingues, I., 2021. Acetylcholinesterase (AChE) activity in embryos of zebrafish. Methods Mol. Biol. 2240, 119–124.

Gu, D., Hong, L., Zhang, L., Liu, H., Shang, S., 2018. Nitrogen and sulfur co-doped highly luminescent carbon dots for sensitive detection of Cd (II) ions and living cell imaging applications. J. Photochem. Photobiol., B 186, 144–151.
Hallare, A.V., Schirling, M., Luckenbach, T., Ko, H., Triebskorn, R., 2005. Combined effects of temperature and cadmium on developmental parameters and biomarker responses in zebrafish. (Danio rerio) embryos 30, 7–17.
Han, C., et al., 2016. Highly fluorescent carbon dots as selective and sensitive "on-off-on" probes for iron(III) ion and apoferritin detection and imaging in living cells. Biosens. Bioelectron. 83, 229–236.
Hartwig, A., 2013. Metal interaction with redox regulation: an integrating concept in metal carcinogenesis? Free Radic. Biol. Med. 55, 63–72.
Herawati, N., Suzuki, S., Hayashi, K., Rivai, I.F., Koyama, H., 2000. Cadmium, copper, and zinc levels in rice and soil of Japan, Indonesia, and China by soil type. Bull. Environ. Contam. Toxicol. 64, 33–39.
Hess, S.C., et al., 2017. Direct synthesis of carbon quantum dots in aqueous polymer solution: one-pot reaction and preparation of transparent UV-blocking films. J Mater Chem A Mater 5, 5187–5194.
Hoang, N.M., et al., 2023a. Experimental synthesis of dual-emission carbon dots: the role of reaction temperature. Inorg. Chem. Commun. 148, 110301.
Hoang, N.M., et al., 2023b. Dual emission carbon dots for simultaneous detections of Pb2+ and Fe3+ ions in water via distinct sensing mechanisms. J. Fluoresc. 33, 1359–1366.
Hoang, N.M., et al., 2025. Multiple functions of carbon dots in rapid removal of potassium permanganate and selective detection of tetracycline. Res. Chem. Intermed. 51, 3939–3952.
Hola, K., et al., 2014. Carbon dots - emerging light emitters for bioimaging, cancer therapy and optoelectronics. Nano Today 9, 590–603.
Hu, G., et al., 2024. Correlation between surface structure of carbon dots and selective detection of heavy metal ions. Appl. Phys. A Mater. Sci. Process. 130, 1–13.
Huang, S., Yang, E., Yao, J., Liu, Y., Xiao, Q., 2018. Red emission nitrogen, boron, sulfur co-doped carbon dots for "on-off-on" fluorescent mode detection of Ag+ ions and l-cysteine in complex biological fluids and living cells. Anal. Chim. Acta 1035, 192–202.
Ikram, M., Haider, A., Moeen, S., Haider, J., 2024. Carbon-based nanomaterials for environmental applications. Engineering Materials **Part** F2893, 1–112.
Järup, L., 2003. Hazards of heavy metal contamination. Br. Med. Bull. 68, 167–182.
Jiao, Y., et al., 2019. One-Step synthesis of label-free ratiometric fluorescence carbon dots for the detection of silver ions and glutathione and cellular imaging applications. ACS Appl. Mater. Interfaces 11.
Jin, J.C., et al., 2018. A novel method for the detection of silver ions with carbon dots: excellent selectivity, fast response, low detection limit and good applicability. Sensor. Actuator. B Chem. 267.
Kakakhel, M.A., et al., 2021. Long-term exposure to high-concentration silver nanoparticles induced toxicity, fatality, bioaccumulation, and histological alteration in fish (Cyprinus carpio). Environ. Sci. Eur. 33, 14.
Khursheed, S., et al., 2023. Biogenic silver nanoparticles: synthesis, applications and challenges in food sector with special emphasis on aquaculture. Food Chem. X 20, 101051.
Kienle, C., Köhler, H.-R., Gerhardt, A., 2009. Behavioural and developmental toxicity of chlorpyrifos and nickel chloride to zebrafish (Danio rerio) embryos and larvae. Ecotoxicol. Environ. Saf. 72, 1740–1747.
Li, C., et al., 2017. The selectivity of the carboxylate groups terminated carbon dots switched by buffer solutions for the detection of multi-metal ions. Sensor. Actuator. B Chem. 240, 941–948.
Li, F., et al., 2023. Adverse effects of silver nanoparticles on aquatic plants and zooplankton: a review. Chemosphere 338, 139459.
Liu, W., et al., 2020. Zebrafish: a promising model for evaluating the toxicity of carbon dot-based nanomaterials. Cite This: ACS Appl. Mater. Interfaces 12, 49020.
López-Beltrán, A., et al., 2023. Design of fluorescent carbon dots (CDs) for the selective detection of metal-containing ions. Chem. Eur J. 29, e202300188.
Masindi, V., Muedi, K.L., Masindi, V., Muedi, K.L., 2018. Environmental contamination by heavy metals. Heavy Metals. https://doi.org/10.5772/INTECHOPEN.76082.
Massarsky, A., et al., 2013a. Assessment of nanosilver toxicity during zebrafish (Danio rerio) development. Chemosphere 92.
Massarsky, A., et al., 2013b. Assessment of nanosilver toxicity during zebrafish (Danio rerio) development. Chemosphere 92, 59–66.
Mauro, N., et al., 2022a. Decagram-scale synthesis of multicolor carbon nanodots: self-tracking nanoheaters with inherent and selective anticancer properties. ACS Appl. Mater. Interfaces 14, 2551–2563.
Mauro, N., et al., 2022b. Decagram-scale synthesis of multicolor carbon nanodots: self-tracking nanoheaters with inherent and selective anticancer properties. ACS Appl. Mater. Interfaces 14, 2551–2563.
Mauro, N., et al., 2022c. Printable thermo- and photo-stable poly(D,L-lactide)/Carbon nanodots nanocomposites via heterophase melt-extrusion transesterification. Chem. Eng. J. 443, 136525.
Mauro, N., et al., 2023. Controlled delivery of sildenafil by β-Cyclodextrin-decorated sulfur-doped carbon nanodots: a synergistic activation of ROS signaling in tumors overexpressing PDE-5. Int. J. Pharm. 645, 123409.
Minh Hoang, N., et al., 2024. Hydrogen bonding effect on pH-sensing mechanism of carbon dots. Inorg. Chem. Commun. 160, 111944.
Mohammad-Jafarieh, P., Akbarzadeh, A., Salamat-Ahangari, R., Pourhassan-Moghaddam, M., Jamshidi-Ghaleh, K., 2021. Solvent effect on the absorption and emission spectra of carbon dots: evaluation of ground and excited state dipole moment. BMC Chem 15.
Morrice, J.R., Gregory-Evans, C.Y., Shaw, C.A., 2018. Modeling environmentally-induced motor neuron degeneration in zebrafish. Sci. Rep. 8.
Nabinger, D.D., et al., 2018. Nickel exposure alters behavioral parameters in larval and adult zebrafish. Sci. Total Environ. 624, 1623–1633.
Nguyen, M.H., et al., 2023. Use of carbon materials for constructing a closed water treatment system. J. Power Sources 573, 233111.
OECD, 2013. OECD Guideline for Testing of Chemicals. Test N236: Fish Embryo Acute Toxicity (FET) Test, 236. 22. Organisation for Economic Co-operation and Development.
Padhye, L.P., et al., 2023. Silver contamination and its toxicity and risk management in terrestrial and aquatic ecosystems. Sci. Total Environ. 871, 161926.
Park, K., Han, E.J., Ahn, G., Kwak, I.S., 2020. Effects of combined stressors to cadmium and high temperature on antioxidant defense, apoptotic cell death, and DNA methylation in zebrafish (Danio rerio) embryos. Sci. Total Environ. 716.
Pereira, S.P.P., Boyle, D., Nogueira, A.J.A., Handy, R.D., 2023. Comparison of toxicity of silver nanomaterials and silver nitrate on developing zebrafish embryos: bioavailability, osmoregulatory and oxidative stress. Chemosphere 336.
Perumal, S., et al., 2022. Simultaneous removal of heavy metal ions using carbon dots-doped hydrogel particles. Chemosphere 286, 131760.
Phetcharee, K., Sirisit, N., Manyam, J., Paoprasert, P., 2021. Highly sensitive Ni2+ sensors based on polyurethane-derived, label-free carbon dots with high adsorption capacity. ChemistrySelect 6, 7964–7971.
R Core Team. R core team, 2021. R: A Language and Environment for Statistical Computing. R Foundation for Statistical Computing, Vienna, Austria. http://www.R-project.org. Preprint at (2021).
Rahmanian, O., Dinari, M., Abdolmaleki, M.K., 2018. Carbon quantum dots/layered double hydroxide hybrid for fast and efficient decontamination of Cd(II): the adsorption kinetics and isotherms. Appl. Surf. Sci. 428.
Rasheed, T., Anwar, M.T., Ferry, D.B., Ali, A., Imran, M., 2023. Zero-dimensional luminescent carbon dots as fascinating analytical tools for the treatment of pharmaceutical based contaminants in aqueous media. Environ. Sci. J. Integr. Environ. Res.: Water Research and Technology 10. https://doi.org/10.1039/d3ew00220a. Preprint at.
Sabet, M., Mahdavi, K., 2019a. Green synthesis of high photoluminescence nitrogen-doped carbon quantum dots from grass via a simple hydrothermal method for removing organic and inorganic water pollution. Appl. Surf. Sci. 463, 283–291.
Sabet, M., Mahdavi, K., 2019b. Green synthesis of high photoluminescence nitrogen-doped carbon quantum dots from grass via a simple hydrothermal method for removing organic and inorganic water pollution. Appl. Surf. Sci. 463.
Santos, C.I.M., et al., 2018. Selective two-photon absorption in carbon dots: a piece of the photoluminescence emission puzzle. Nanoscale 10, 12505–12514.
Scott, G.R., Sloman, K.a., 2004. The effects of environmental pollutants on complex fish behaviour: integrating behavioural and physiological indicators of toxicity. Aquat. Toxicol. 68, 369–392.
Simões, R., Rodrigues, J., Neto, V., Monteiro, T., Gonçalves, G., 2024. Carbon dots: a bright future as anticounterfeiting encoding agents. Small 20. https://doi.org/10.1002/smll.202311526. Preprint at.
Tan, Q., et al., 2022. One-step synthesis of highly fluorescent carbon dots as fluorescence sensors for the parallel detection of cadmium and mercury ions. Front. Chem. 10, 1005231.
Tang, F.H.M., Lenzen, M., McBratney, A., Maggi, F., 2021. Risk of pesticide pollution at the global scale. Nat. Geosci. 14 (4 14), 206–210, 2021.
Torres Landa, S.D., Reddy Bogireddy, N.K., Kaur, I., Batra, V., Agarwal, V., 2022. Heavy metal ion detection using green precursor derived carbon dots. iScience 25, 103816.
Tran, N.-A., et al., 2023a. Carbon dots in environmental treatment and protection applications. Desalination 548, 116285.
Tran, N.A., et al., 2023b. Carbon dots in environmental treatment and protection applications. Desalination 548. https://doi.org/10.1016/j.desal.2022.116285. Preprint at.
Umar, E., et al., 2023. A state-of-the-art review on carbon quantum dots: prospective, advances, zebrafish biocompatibility and bioimaging in vivo and bibliometric analysis. Sustain. Mater. Technol. 35.
Van Aerle, R., et al., 2013a. Molecular mechanisms of toxicity of silver nanoparticles in zebrafish embryos. Environ. Sci. Technol. 47, 8005–8014.
Van Aerle, R., et al., 2013b. Molecular mechanisms of toxicity of silver nanoparticles in zebrafish embryos. Environ. Sci. Technol. 47, 8005–8014.
Venables, W.N., Ripley, B.D., 2002. Modern Applied Statistics with S Fourth Edition by, 53. World.
Vrèek, I.V., Šinko, G., 2013. Inactivation of cholinesterases by silver and gold ions in vitro. Cent. Eur. J. Chem. 11, 935–944.
Wang, Y., Zhu, Y., Yu, S., Jiang, C., 2017a. Fluorescent carbon dots: rational synthesis, tunable optical properties and analytical applications. RSC Adv. 7, 40973–40989.
Wang, Y., Zhu, Y., Yu, S., Jiang, C., 2017b. Fluorescent carbon dots: rational synthesis, tunable optical properties and analytical applications. RSC Adv. 7. https://doi.org/10.1039/c7ra07573a. Preprint at.
Wang, Y. Te, Wu, R.R., Zhang, Y.Y., Cheng, S.R., Zhang, Y., 2023. High quantum yield nitrogen doped carbon dots for Ag+ sensing and bioimaging. J. Mol. Struct. 1283, 135212.
Wright, D.A., Welbourn, P.M., 1994. Cadmium in the aquatic environment: a review of ecological, physiological, and toxicological effects on biota. Environ. Rev. 2, 187–214.
Xu, Y., et al., 2022a. Developmental exposure to environmental levels of cadmium induces neurotoxicity and activates microglia in zebrafish larvae: from the perspectives of neurobehavior and neuroimaging. Chemosphere 291.
Xu, X.J., et al., 2022b. Fluorescent carbon dots for sensing metal ions and small molecules. Chin. J. Anal. Chem. 50, 103–111.
Yang, H., et al., 2019. Hydrophobic carbon dots with blue dispersed emission and red aggregation-induced emission. Nat. Commun. 10, 1789.

Zhang, B., et al., 2017. Effects of three different embryonic exposure modes of 2, 2′, 4, 4′-tetrabromodiphenyl ether on the path angle and social activity of zebrafish larvae. Chemosphere 169, 542–549.
Zhang, Q., et al., 2022. Green synthesis of mustard seeds carbon dots and study on fluorescence quenching mechanism of Fe3+ ions. Inorg. Chem. Commun. 146, 110034.
Zhou, Y., Shi, J., Ning, J., Hu, G., Zhou, Y., 2023. Carbon dots-based modularization fluorescent probe for simultaneous detection of Hg2+ and Cu2+ in water, cells and zebrafish. Dyes Pigments 214, 111232.
Zhu, W., et al., 2022. Screening of multifunctional fruit carbon dots for fluorescent labeling and sensing in living immune cells and zebrafishes. Microchim. Acta 189, 1–13.
Zu, F., et al., 2017. The quenching of the fluorescence of carbon dots: a review on mechanisms and applications. Microchim. Acta 184, 1899–1914.